

**CONVERSION OF COCONUT OIL DERIVED METHYL ESTERS INTO
NITROGEN COMPOUNDS AS GREEN CORROSION INHIBITOR**

(Skripsi)

By

ALYA IKA NUR AFIFAH



**FACULTY OF MATHEMATICS AND NATURAL SCIENCES
UNIVERSITY OF LAMPUNG
BANDAR LAMPUNG
2023**

ABSTRACT

CONVERSION OF COCONUT OIL DERIVED METHYL ESTERS INTO NITROGEN COMPOUNDS AS GREEN CORROSION INHIBITOR

By

ALYA IKA NUR AFIFAH

This study was carried out as an attempt to convert methyl esters derived from coconut oil into nitrogen compounds by reacting the methyl esters with diethanolamine. To produce methyl ester, coconut oil was refluxed with methanol at 70 °C for 3 hours in the presence of zeolite-A catalyst. To produce nitrogen compounds, three samples were prepared by carrying out experiment in an autoclave then heated in an oven at 80 °C for 24 hours, at 100 °C for 24 and 48 hours. The products of the reactions were analyzed using GC-MS and FTIR, then utilized as corrosion inhibitor for mild steel in CO₂ saturated brine solution using Wheel test method. The inhibition activity of the samples was evaluated in terms of percentage protection and surface morphology of the sample using SEM-EDX method. The experimental results obtained revealed that the experiments conducted at 80 °C for 24 hours and at 100 °C for 24 hours only produced nitrogen compounds as a minor component, but in the sample produced from the experiment carried out 100 °C for 48 hours, a series of nitrogen compounds were produced, contributing 53.54% to the composition. The results of corrosion testing experiments revealed that the samples exhibit corrosion inhibition activity, with the highest protection of 97.9% was provided by the sample prepared at 100 °C for 48 hours. Without ignoring the need for further research, the results obtained in this study suggest that the nitrogen compounds derived from coconut oil possess promising potential as green corrosion inhibitor.

Keywords: zeolite-A, coconut oil methyl ester, nitrogen compounds, corrosion inhibitor, and wheel test.

**CONVERSION OF COCONUT OIL DERIVED METHYL ESTERS INTO
NITROGEN COMPOUNDS AS GREEN CORROSION INHIBITOR**

By

ALYA IKA NUR AFIFAH

Skripsi

**As One of The Requirement For The Degree
SARJANA SAINS**

At

**Department of Chemistry
Faculty of Mathematics and Natural Sciences**



**FACULTY OF MATHEMATICS AND NATURAL SCIENCES
UNIVERSITY OF LAMPUNG
BANDAR LAMPUNG
2023**

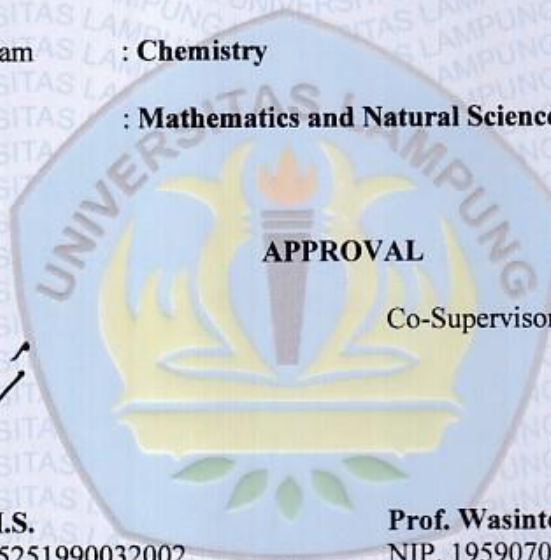
Research Title : **CONVERSION OF COCONUT OIL DERIVED METHYL ESTERS INTO NITROGEN COMPOUNDS AS GREEN CORROSION INHIBITOR**

Student Name : *Alya Ika Nur Afifah*

Student ID : **1817011062**

Study Program : **Chemistry**

Faculty : **Mathematics and Natural Sciences**



Supervisor

Dr. Ilim, M.S.
NIP. 196505251990032002

Co-Supervisor

Prof. Wasinton Simanjuntak, Ph.D.
NIP. 195907061988111001


Head of Department

Mulyono, Ph.D.
NIP.197406112000031002


AUTHORIZE

1. Examiner Team

Chief : **Dr. Ilim, M.S.**



Secretary : **Prof. Wasinton Simanjuntak, Ph.D.**



Examiner
Non Supervisor : **Prof. Sutopo Hadi, M.Sc.**



2. Dean of Faculty of Mathematics and Natural Sciences



Dr. Eng. Suropto Dwi Yuwono, M.T.
NIP: 197407052000031001



Date of the examination : **11st January 2023**

STATEMENT OF AUTHORSHIP

The undersigned:

Name : Alya Ika Nur Afifah
Student ID : 1817011062
Department : Chemistry
Faculty : Mathematics and Natural Sciences
University : University of Lampung

Truly declare that my final project report entitled **“Conversion of Coconut Oil Derived Methyl Esters Into Nitrogen Compounds as Green Corrosion Inhibitor”** is truly my own work, both the ideas, results, and analysis. Furthermore, I also have no objection if some or all of the data in this final project report are used by the lecturer or department for publication purposes, as long as my name is mentioned and there is an agreement prior to publication.

Bandar Lampung, 11st January 2023

The Author



Alya Ika Nur Afifah
Student ID. 1817011062

AUTHOR'S BIOGRAPHY



The author's full name is Alya Ika Nur Afifah. The author was born in Magelang, on July 9th 2001. The author is the first daughter of Mr. Alip Muhtarom and Mrs. Haryani. The author lives in Rajeg district, Tangerang, Banten.

The author graduated from TK Al-Muhsinin Kab. Tangerang on 2006, elementary school at SD Islam Terpadu Bani Yahya Soleman Kab. Tangerang on 2012, junior high school at SMP Negeri 1 Sepatan Kab. Tangerang on 2015, and senior high school at SMA Negeri 11 Kabupaten Tangerang on 2018. The author was enrolled as student in Department of Chemistry, Faculty of Mathematics and Natural Sciences, University of Lampung from SBMPTN test on July 2018. The author joined the physical chemistry peer group for final project.

During the study in Department of Chemistry, the author was attended in Himpunan Mahasiswa Kimia (Himaki) as member of Bidang Kaderisasi dan Pengembangan Organisasi (KPO) on 2019-2020. The author was attended the internship at PT Bukit Asam Tbk. Unit Pelabuhan Tarahan as coal analyst on February – March 2021. On August – September 2021, the author was attended the community service program called Kuliah Kerja Nyata (KKN) in Kelurahan Gebang Raya, Tangerang, Banten.

The author was also joined some of international seminar as presenter, such as The 4th International Conference on Applied Sciences, Mathematics, and Informatics (ICASMI) entitled "Application of Zeolite-A as Catalyst For Conversion of Coconut Oil Into Nitrogen Compounds as Green Corrosion

Inhibitor” on September 2022 and The 12th International Conference on Green Technology (ICGT) with entitled “The Study on Corrosion Inhibitor Activities of Nitrogen Compounds Derived From Coconut Oil Methyl Ester Using Autoclave Method” on October 2022.

This scientific work is dedicated entirely to the people I love:

My beloved parents
Mr. Alip Muhtarom and Mrs. Haryani

My beloved brother
Akmal Nur Ihsan

My supervisors
Dr. Ilim, M.S.
Prof. Wasinton Simanjuntak, Ph.D.

All of the lecturers in Department of Chemistry

My beloved friends

My beloved almamater
University of Lampung

MOTTO

يَا أَيُّهَا الَّذِينَ آمَنُوا إِذَا قِيلَ لَكُمْ تَفَسَّحُوا فِي الْمَجَالِسِ فَافْسَحُوا
يَفْسَحَ اللَّهُ لَكُمْ وَإِذَا قِيلَ انشُرُوا فَانشُرُوا يَرْفَعِ اللَّهُ الَّذِينَ آمَنُوا
مِنْكُمْ وَالَّذِينَ أُوتُوا الْعِلْمَ دَرَجَاتٍ ۗ وَاللَّهُ بِمَا تَعْمَلُونَ خَبِيرٌ

O you who have believed, when you are told, “space yourselves” in assemblies, then make space; Allah will make space for you. And when you are told, “arise,” then arise; Allah will raise those who have believed among you and those who were given knowledge, by degrees. And Allah is Acquainted with what you do.

[Al Mujaadila 58:11]

“All humans are dead except those who have knowledge; and all those who have knowledge are asleep, except those who do good deeds; and those who do good deeds are deceived, except those who are sincere; and those who are sincere are always in a state of worry.”

[Imam Shaafi'i]

Treat People with Kindness

[Harry Styles]

Cool Kids Don't Dance

[One Direction]

ACKNOWLEDGEMENTS

By the name of Allah Almighty, the Lord of the world, who has been giving the author His guidance, mercy, blessing, and health to complete this academic requirement. Shalawat and salam are forever for a noble character, the prophet Muhammad SAW., who has brought the human beings from the darkness to the lightness and from the bad character to the good one.

Alhamdulillah rabbi 'alamin, the author could be completed this final project report with the entitle "Conversion of Coconut Oil Derived Methyl Esters Into Nitrogen Compounds as Green Corrosion Inhibitor". In this occasion, the author would like to express the great thanks to:

1. My beloved parents, Mr. Alip Muhtarom and Mrs. Haryani. Thank you so much for the never-ending supports, a lot of love and care, thank you for being my inspiration. May Allah give both of you limitless healthy, patience, and His blessings.
2. My hunny bunny little brother Akmal Nur Ihsan. Thank you for being with Mom and Dad during the period I finished my study in Lampung. Thank you for always entertaining and support me to finish my study. May Allah give you His blessings.
3. Dr. Ilim, M.S. as my supervisor. Thank you for the guidance, motivation and advice to the author for completing this final project report.
4. Prof. Wasinton Simanjuntak, Ph.D. as my co-supervisor. Thank you for the guidance, motivation and advice to the author for completing this final project report.
5. Prof. Sutopo Hadi, M.Sc. as my examiner. Thank you for the guidance, motivation and advice to the author from the beginning proposal until the final report.

6. Dr. Eng. Suripto Dwi Yuwono, M.T. as the Dean of Faculty of Mathematics and Natural Sciences.
7. Mulyono, Ph.D. as the Head of Chemistry Department FMIPA Unila.
8. Dr. Mita Rilyanti, M.Si. as the Secretary of Chemistry Department and also my academic supervisor. Thank you for the suggestion and motivation to the author from the start period of my study.
9. All of the lecturers of Chemistry Department who have given their knowledge, information, and insight both through formal classroom meeting and through informal occasional one.
10. My research partner “Barisan Pelopor” Alhuda Fidyati Vazira, Nabila Anastasya, and Sahrul Junaidi. Thank you for the support, help, love, laugh and the unforgettable experience during our research.
11. Corrosion Research Team, Mba Elin, Mba Laila, Arya, Ditto, Rifdah, and Devy. Thank you for the support, help, love, and laugh. Cheers to another moments together in another places.
12. Polymer Lab 2022, Annida, Anggun, Aryani, Randi, Chori, Elis, Mba Tika, Mba Diska, Eki, Zahra, Quntum, Rangga, Tio, Erika, and Selvia. Thank you for the support and help during my research in laboratory.
13. My partner of the year Afifa Nabilla Mutiq, you are truly my partner in everything. Thank you for the support, help, love, laugh, and cry together through this hard college and research life.
14. Salsabila and Salsabilla Bethari Purworini, who always being here, by my side, since the first we met at PKKMB. We have been through this, thank you for the love and laugh since 4 years ago, and many more years ahead.
15. My beloved friends in Chemistry Department Batch 2018, thank you for the meaningful experience we have been through together for the last 4 years. See you guys on top.
16. Siti Auliasyifa, my beloved partner in everything since we were high school. Thank you for always supporting me since the beginning and pushed me to get the Bachelor’s Degree in 2022.
17. Jason Joshua and Fachri Muhammad. My KKN partner and also my step brothers. Thank you for always being my brother since the time we met at

Gebang Raya until now. Thank you for being the part of my life, thank you for being my side when I was settle down.

18. My beloved friends since middle school Tiwi, Suryo, Nando, Amel, and Yuli. Thank you for the support, love, and laugh until now. Thank you for always entertaining me with the random chat.
19. Last but not least, M. Rifki Fadillah and his beloved family. Thank you for the support, love, laugh, cry, mad, confused, and cheerful moments we have been through together. Thank you for the motivation you gave to me every single day we met.

Finally, the writer really realizes that are many weaknesses in this final project report. Therefore, constructive critiques and suggestion are needed in order to improve this report. May Allah Almighty bless you, bless me, and bless us. Aamin Yaa Rabbal ‘Alamin.

Bandar Lampung, January 2023

The Author

Alya Ika Nur Afifah

TABLE OF CONTENTS

	Pages
LIST OF TABLES	ix
LIST OF FIGURES	x
I. INTRODUCTION	1
1.1. Background.....	1
1.2. Research Purposes	3
1.3. Research Benefits	3
II. LITERATURE REVIEW	4
2.1. Corrosion	4
2.2. Mechanism of Metal Corrosion.....	4
2.3. Types of Corrosion	5
2.4. CO ₂ Corrosion	6
2.5. Corrosion Control.....	7
2.6. Corrosion Inhibitor	9
2.6.1. Inorganic Inhibitors	9
2.6.2. Organic Inhibitors.....	9
2.7. Derivatives of Coconut Oil.....	10
2.7.1. Methyl Ester of Coconut Oil	10
2.7.2. Nitrogen Compounds.....	11
2.8. Zeolite-A.....	12
2.9. Characterization of Products	14
2.9.1. X-Ray Diffraction (XRD).....	14

2.9.2. Scanning Electron Microscopy with Energy Dispersive X-ray (SEM-EDX).....	16
2.9.3. Fourier Transform Infrared (FTIR)	17
2.9.4. Gas Chromatography–Mass Spectrometry (GC–MS).....	20
2.10. Corrosion Rate Measurement	21
2.10.1. Weight Loss Method (Wheel Test)	22
2.10.2. Electrochemical Methods	22
III. RESEARCH METHODS.....	26
3.1. Time and Places	26
3.2. Materials and Instruments	26
3.3 Research Procedures	27
3.3.1 Preparation of Rice Husk.....	27
3.3.2. Extraction of Rice Husk Silica	27
3.3.3. Synthesis of Zeolite-A Catalyst.....	27
3.3.4. Transesterification of Coconut Oil	28
3.3.5. Reaction Between Methyl Ester and Diethanolamine.....	28
3.3.6. Preparation of Mild Steel.....	29
3.3.7. Preparation of Solutions	29
3.3.8. Corrosion Rate Measurement	30
3.3.9. Scanning Electron Microscopy with Energy Dispersive X-Ray (SEM-EDX).....	30
IV. RESULTS AND DISCUSSIONS.....	31
4.1. Scope of The Study.....	31
4.2. Extraction of Rice Husk Silica	31
4.3. Preparation and Characterization of Zeolite-A.....	32
4.4. Transesterification Reaction and Characterization of Product	34
4.5. Reaction Between Methyl Ester and Diethanolamine and Characterization of The Product.....	38
4.6. Corrosion Rate Measurement Using Wheel Test	43
4.7. Surface Characterization Using SEM-EDX	44

V. CONCLUSIONS AND SUGGESTIONS.....	47
5.1. Conclusions	47
5.2. Suggestions.....	48
REFERENCES.....	49
ATTACHMENTS	57
Attachment 1. Extraction of rice husk silica.....	58
Attachment 2. Calculation of zeolite-A composition	59
Attachment 3. Calculation of percent conversion	61
Attachment 4. Mass spectrum of methyl esters	62
Attachment 5. Mass spectrum of nitrogen compounds	64
Attachment 6. Calculation of preparation solutions	66
Attachment 7. Calculation of wheel test method.....	68

LIST OF TABLES

Tables	Pages
1. Fatty acids content in coconut oil	10
2. Range in wavenumber (cm^{-1}) of each functional groups	18
3. Chemical composition of mild steel SAE/AISI Grade 1022	29
4. Comparison of the XRD data for zeolite-A standard IZA and synthesized zeolite-A.....	33
5. The components of methyl ester coconut oil	36
6. Components identified of P-1	40
7. Components identified of P-2	41
8. Components identified of P-3	42
9. The results of the wheel test using P-1, P-2, and P-3 as inhibitor	43
10. Dimensions of mild steels and percent protections data.....	68

LIST OF FIGURES

Figures	Pages
1. Corrosion schematic of metal	4
2. Transesterification of lauric acid into methyl laurate	11
3. Amidation reaction from: a) fatty acid and b) methyl ester	12
4. Structure of zeolite-A.....	13
5. Schematic diagram of a diffractometer system.....	15
6. XRD Pattern of Zeolite-A.....	15
7. Scanning Electron Microscopy (SEM) components.....	16
8. Micrograph of zeolite-A.....	17
9. An example of FTIR spectrum of coconut oil methyl ester.....	19
10. Instrumentation of the double-beam (top) and single-beam (bottom) IR spectrophotometers.	20
11. Scheme of GC–MS	21
12. A scheme of EIS circuit and the redox reaction takes place at the surface of working electrodes in an electrochemical cell	23
13. Nyquist plot with impedance vector	24
14. Electrochemical equivalent circuit used to fit the impedance spectra	24
15. Tafel slope from potentiodynamic polarization	25
16. Diffractogram of synthesized zeolite-A compared to zeolite-A IZA	32
17. Micrograph of synthesized zeolite-A.....	34
18. FTIR spectra of methyl ester coconut oil.....	35
19. Chromatogram of methyl ester coconut oil	36

20. Mass spectrum of methyl laurate	37
21. Fragmentation pattern of methyl laurate	37
22. FTIR spectrum of methyl ester, P-1, P-2, and P-3	39
23. Chromatogram of P-1	40
24. Chromatogram of P-2	41
25. Chromatogram of P-3	42
26. Micrographs of the mild steel samples investigated	45
27. The elemental composition of the sample detected using EDX	46
28. Extraction of rice husk silica	58
29. Mass spectrum of methyl caprylate	62
30. Mass spectrum of methyl caprate	62
31. Mass spectrum of methyl laurate.	62
32. Mass spectrum of methyl miristate.	62
33. Mass spectrum of methyl palmitate.	63
34. Mass spectrum of methyl oleate	63
35. Mass spectrum of methyl stearate	63
36. Mass spectrum of tripropylamine	64
37. Mass spectrum of hexanamide, N-(2-hydroxyethyl)-	64
38. Mass spectrum of caprylic acid monoethanol amide.	64
39. Mass spectrum of decanamide, N-(2-hydroxyethyl)-	64
40. Mass spectrum of lauric diethanolamide	65
41. Mass spectrum of 1-piperazineethanol	65

I. INTRODUCTION

1.1. Background

Metals are very important materials used in many applications, from simple daily tools or utensils to structural applications. Despite their flexibility and strength, some metals are prone to corrosion; one of them is iron or iron alloy such as mild steel. Corrosion of mild steel remains a challenging problem since this type of metal is a prominent structural material, including underground piping systems such as in oil and gas industry. Corrosion is the surface disintegration of metals or alloys due to their contact with corrosive species within specific environments. From chemistry point of view, corrosion is electrochemical reaction in which the metal is oxidized by corrosive species, converting the metal into cationic species. The cationic species then leaves the surface of the metal, exposing the surface to a new oxidation reaction.

To suppress corrosion, several protection methods have been developed, with the most widely applied are coatings, electrochemical protection (anodic or cathodic protection), and the use of corrosion inhibitors. Of all these techniques, the use of corrosion inhibitor is considered as the most cost effective and the easiest to apply. Corrosion inhibitors are chemical compounds that in small quantities can retard the degradation of metals in hostile environments (Musa *et al.*, 2012). In a broad sense, corrosion inhibitors are distinguished into inorganic and organic inhibitors. Several examples of inorganic inhibitors are chromates (Garai *et al.*, 2012), polyphosphates (Jiang *et al.*, 2018), and benzothiazole (Salarvand *et al.*, 2016). In spite of their good performance, inorganic inhibitors are generally expensive and some of them are toxic and harmful to the environment and human health (Qiang *et al.*, 2018). As a consequence, the use of organic inhibitors is

preferred over inorganic inhibitors. Organic inhibitors can be classified as natural and synthetic, however synthetic inhibitors are more widely applied, mainly for availability and effectivity reasons.

Organic inhibitors have been widely used due to the ability of these compounds to prevent corrosion in various corrosive environments. Typically, effective organic inhibitors contain either N, S, or O atoms in their structures or electronegative functional groups and π electrons in triple or conjugated double bonds, because these atoms and the functional groups can be adsorbed on metal surface via coordinate covalent bond or via electrostatic interaction between the metal surface and inhibitor. As the results, inhibitor can form a protective layer which covers the metal surface. This protective layer prevents or limits the contact between the metal surface and corrosive species present in the environment (Alvarez *et al.*, 2017). Typical examples of nitrogen containing organic inhibitors that have been reported to exhibit good performance to protect mild steel against CO₂ corrosion in brine solution are the oligomers of 4-vinylpyridine (Ilim *et al.*, 2016), oligomer 4-vinylpiperidine (Ilim *et al.*, 2017), and oligomer 2-vinylpyridine (Ilim *et al.*, 2021).

Another trending focus of corrosion inhibitor is development of green corrosion inhibitor. In this respect, in previous study (Herliana, 2022) preparation of nitrogen compounds was attempted by reacting methyl esters derived from coconut oil with diethanolamine. In the study, the experiment was carried out by refluxing the mixture in the presence of zeolite-A as catalyst. The study shows that the addition of 150 ppm inhibitor at 50 °C has inhibition efficiency (percent protection) of 58.8% (wheel test), 88% (EIS), and 83% (Tafel plot). However, the only methyl ester that has been successfully converted into nitrogen compound is methyl laurate to lauryl diethanolamide. In addition, the amidation product is still containing other components such as glycerin, unreacted diethanolamine, and remaining methyl esters. In the study, the relative amount of nitrogen compounds formed is 40.30% which indicates that need to improve the method in order to optimize the production of nitrogen compounds.

In attempt to improve the method, in this study preparation of nitrogen compounds was conducted by two steps. In the first step, coconut oil was reacted with methanol (transesterification) in the presence of zeolite-A prepared from rice husk silica and aluminum foil as catalyst, to produce methyl esters. The methyl esters were then mixed with diethanolamine and zeolite-A, and the mixture was transferred into a Teflon lined autoclave. The autoclave was then placed in an oven set at specified temperature and held for specified time. After the completion of the reaction, the product was characterized using FTIR and GC-MS. Finally, the product tested as corrosion inhibitor for mild steel by wheel test method.

1.2. Research Purposes

The purposes of this research are:

1. To produce methyl esters of coconut oil.
2. To produce nitrogen compounds derived from methyl esters of coconut oil.
3. To obtain experimental data showing the performance of the nitrogen compounds as corrosion inhibitor for mild steel.

1.3. Research Benefits

In addition to enrichment of science and technology, green corrosion inhibitor in particular, this study will promote generation of value added from rice husk silica and to increase the economic value of coconut oil.

II. LITERATURE REVIEW

2.1. Corrosion

Corrosion is the destruction of a material, especially metals due to a chemical reaction between the material and its environment. Corrosion is a process that occurs naturally and continuous to proceed as long as the metal remains in a corrosive environment (Yanuar *et al.*, 2016). In the oil, gas, and chemical industries, corrosion is one of the most challenging tasks, and its reported that in USA corrosion costs 170 billion USD per year (Dwivedi *et al.*, 2017), due to various corrosion impacts such as failure in components, depletion of natural resources including metals, and unpleasant appearance of the corroded materials.

2.2. Mechanism of Metal Corrosion

Mechanism of metal corrosion can be considered as chemical reaction in which metal undergoes oxidation as show in Figure 1.

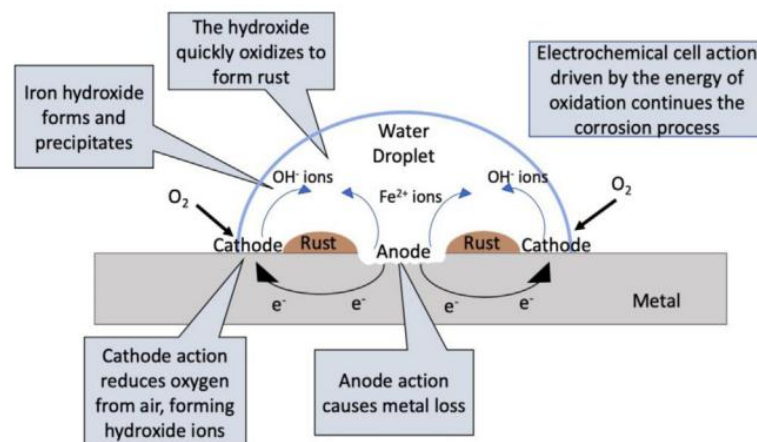


Figure 1. Corrosion schematic of metal (Koushik *et al.*, 2021).

Based on Figure 1, water droplet can interact with metal surface and leading to the losses of metal. Metal such as iron (Fe) can be oxidized into Fe^{2+} cation and dissolve easily in the water. The area where oxidation took places called anode. This oxidation reaction occurs according to Equation (1):



Further oxidation of iron causes pits on the surface. Oxygen (O_2) from the air can interact with the edge of water droplet, leading to reduction and undergoes reaction to produce hydroxide ions. This reaction took places in cathode as indicated in Equation (2):



The Fe^{2+} ions as product from oxidation in anode region and hydroxide ions (OH^{-}) as product of reduction in cathode region can react to form solid $\text{Fe}(\text{OH})_2$ on the surface on Fe metal. This $\text{Fe}(\text{OH})_2$ also known as rust.

2.3. Types of Corrosion

Based on the types of deterioration of the material, corrosion can be classified as uniform corrosion, crevice corrosion, pitting corrosion, intergranular corrosion, and galvanic corrosion. Uniform corrosion is a corrosion that leads to gradual loss of the surface of the material, leading to reduction of the thickness of the material uniformly. This type of corrosion is commonly encountered for active metals, such as Fe and Zn. For aluminum, uniform corrosion is less significant since this metal can form protective layer in the form of oxide on the surface of the metal (Rufino *et al.*, 2010).

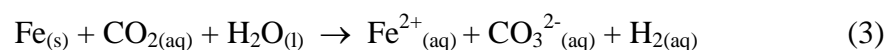
Crevice corrosion, is a corrosion that leads to formation of crevice on the surface of material which can be penetrated by corrosive agents, such as acidic or alkaline solutions, making the crevice regions become highly corrosive and lead to the material decomposition (Chen *et al.*, 2016). Pitting corrosion occurs on the surface of materials and forms small holes which difficult to detect, making it, as the most hazardous form of corrosion. It happens on passivated materials and

alloys in specific environments containing reactive ions such as iodide and chloride ions (Aghuy *et al.*, 2015).

Intergranular corrosion, includes enhanced rust or lateral disintegration of the grain boundaries of the material, although the surface is not rusted. Intergranular corrosion attacks the microstructural grains of the material, leading to loss of toughness, reduction of the ability to withstand tensile stress, and unnoticed fracture (Zhang *et al.*, 2017). Galvanic corrosion, is a type of corrosion that happens between two different metals in contact with each other either indirectly or directly. It can also happen between other conducting materials like graphite, metals, and alloys. In this type of corrosion, a galvanic couple forms between two metals, where one metal becomes the anode and the other becomes the cathode. As a result, the metal which acts as an anode will corrode faster, while the cathode deteriorates more slowly. Galvanic corrosion occurs if different metals are electrochemically in contact in the presence of electrolyte such as water (Håkansson *et al.*, 2017).

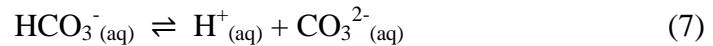
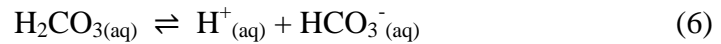
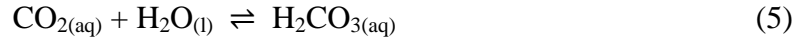
2.4. CO₂ Corrosion

CO₂ corrosion is one of the major concerns in the oil and gas industry. CO₂ corrosion of carbon steel represents a phenomenon occurring when CO₂ dissolves in water and hydrates to become carbonic acid (H₂CO₃), which influences solution pH and provides cathodic species for reaction with the metal pipe surface. CO₂ corrosion of carbon steel is an electrochemical process that involves the anodic dissolution of iron and the cathodic evolution of hydrogen. The overall reaction can be expressed in Equation (3):



A number of chemical, electrochemical, and transport processes occur simultaneously in aqueous CO₂ corrosion of mild steel. The first step is the dissolution of gaseous carbon dioxide in water, as described in Equation (4). The second step is the hydration of aqueous CO₂, which results in the formation of

carbonic acid (H_2CO_3) as shown in Equation (5). The carbonic acid can release hydrogen ions as shown in Equation (6) and Equation (7). This process is relatively slow and is often the rate-determining step in CO_2 corrosion (Kahyarian *et al.*, 2017). The sequence of reactions associated with the presence of CO_2 in H_2O is as follows:



CO_2 corrosion can be reduced by the formation of a thin film of organic inhibitors on the surface of the steel, or a protective corrosion product layer such as iron carbonate. These processes form a protective barrier on the metal surface based on the mechanism of adhesion to the metal surface.

2.5. Corrosion Control

Corrosion control is achieved by recognizing and understanding corrosion mechanisms, using corrosion-resistant materials and altering designs, also by using protective systems, devices, and treatments. Forms of corrosion protection include material selection, coatings, cathodic protection, anodic protection, and the use of inhibitors (Pampliega *et al.*, 2014).

The proper selection and usage of material can reduce the effects of corrosion. The advances in composite materials initiated the shift toward the selection of more composite materials from the earlier trends of performing the studies on mild steel. The introduction of modern composite materials such as nickel aluminum bronze alloy is an example of the change in material selection. The study on the effects of alloying elements in corrosion is an important step toward the advancement in corrosion studies (Kuruvila *et al.*, 2018). However, the selection of materials used to reduce corrosion is expensive, so other methods are preferred.

Metallic, inorganic and organic coatings are used frequently for providing long-term corrosion protection of metals in various types of corrosive media. There are two main types of coatings: barrier coatings and sacrificial coatings. A barrier coating acts as a shield and protects the metal from the surrounding environment, whereas a sacrificial coating functions as a sacrificial anode and thus, corrodes preferentially. Barrier coatings are typically unreactive, resistant to corrosion, and protective against wear. Sacrificial coatings provide cathodic protection by supplying electrons to the base metal (Tator, 1997). Coating pigments commonly used to reduce corrosion containing lead and chromate which are toxic and bad for environment (Costa and Klein, 2006). Therefore, other methods are preferred to reduce corrosion.

Cathodic protection is a widely used electrochemical method for protecting a structure or important components of a system from corrosion. The principle behind cathodic protection is that dissolution of a metal (cathode) can be suppressed by supplying it with electrons, and in effect, controlling the corrosion. Corrosion is then targeted on the anode instead of the metal. Since an electrolyte is required for this method of protection, cathodic protection is not effective for systems in air or other environments that resist current flow between the anode and cathode (Fontana, 2000).

Anodic protection is a method of corrosion control that was developed more recently than cathodic protection, but it is used less frequently. The principle of anodic protection involves passivation of the metal to be protected. A passive film forms on the surface of the metal with the application of an electrical current. Once this film is formed, it acts to protect the metal from dissolution, and the film itself is nearly insoluble in the environment which it formed. Passivation causes metals to become very non-reactive and consequently very resistant to corrosion (Locke, 1997).

2.6. Corrosion Inhibitor

The use of corrosion inhibitor to reduce corrosion is considered as the most cost effective and the easiest to apply. Corrosion inhibitor is a chemical compound which is added in small quantity in solutions or gas can reduce corrosion rate of metals or alloys. Corrosion inhibitor reduces corrosion rate by formation of a film which inhibit corrosion process on the metal surface. The other mechanism is by increasing solution resistivity to reduce corrosion rate (Asmara *et al.*, 2018). Corrosion inhibitors are distinguished into inorganic and organic inhibitors.

2.6.1. Inorganic Inhibitors

Inorganic corrosion inhibitors contain the salts of zinc, copper, nickel, arsenic, and additional metals, with the arsenic compounds being the ones that are most commonly used. There are advantages as well as disadvantages when using the inorganic inhibitors. The advantages are they work excellently at high temperatures for longer periods and are less expensive than organic inhibitors. Inorganic inhibitors are more likely to lose their grip in acid solutions that are stronger than 17% hydrochloric acid, tougher to combine, and might release toxic arsine gas as the product of corrosion (Tamalmani and Husin, 2020). The use of inorganic inhibitors, particularly those containing phosphate, chromate, and other heavy metals, is now being restricted or banned by various environmental regulations because of their toxicity in their disposal especially in the marine industry, where aquatic life is at threat (Roy *et al.*, 2014).

2.6.2. Organic Inhibitors

Organic compounds that consist of nitrogen, oxygen, and/or sulfur are considered as competent industrial corrosion inhibitors (Goyal *et al.*, 2018). Their effectiveness depends on the chemical composition, their molecular structure, and their affinities for the metal surface. High inhibition effectiveness of organic inhibitors are linked with their highly electron rich adsorption centers. Generally,

polar functional groups such as $-\text{OH}$, $-\text{CN}$, $-\text{NH}_2$, $-\text{NO}_2$, $-\text{CONH}_2$, $-\text{COOC}_2\text{H}_5$, and $\text{NH}-\text{SO}_2-$, and extended conjugation in the form of homo and hetero-atomic double ($-\text{C}=\text{C}$, $\text{C}=\text{O}$, $-\text{C}=\text{N}-$ and $-\text{N}=\text{N}-$) and triple bonds ($-\text{C}\equiv\text{N}$, $-\text{C}\equiv\text{NC}-$) act as adsorption centers. The interactions between organic inhibitors results the adsorption and formation of surface film and protect metal from corrosion (Verma *et al.*, 2019). Implementation of organic corrosion inhibitors is the most significant methods due to its several beneficial properties such as easy to synthesis, easy to application, cost-effective, and high inhibition performance (Adejo *et al.*, 2019). One of the organic inhibitor have been used is oligomer 4-vinylpyridine against CO_2 corrosion for mild steel (Ilim *et al.*, 2021). In the study, oligomer 4-vinylpyridine showed exhibited corrosion inhibitor activity in wheel test method and the protection was confirmed by EIS and Tafel analysis results which 81.9% and 87.8% respectively.

2.7. Derivatives of Coconut Oil

2.7.1. Methyl Ester of Coconut Oil

Coconut oil is composed of various fatty acids as presented in Table 1.

Table 1. Fatty acids content in coconut oil

Fatty acid	Chemical Formula	Amount (%)
Caprylic acid	$\text{C}_8\text{H}_{16}\text{O}_2$	8
Capric acid	$\text{C}_{10}\text{H}_{20}\text{O}_2$	7
Lauric acid	$\text{C}_{12}\text{H}_{24}\text{O}_2$	49
Myristic acid	$\text{C}_{14}\text{H}_{28}\text{O}_2$	8
Palmitic acid	$\text{C}_{16}\text{H}_{32}\text{O}_2$	8
Stearic acid	$\text{C}_{18}\text{H}_{36}\text{O}_2$	2
Oleic acid	$\text{C}_{18}\text{H}_{34}\text{O}_2$	6
Linoleic acid	$\text{C}_{18}\text{H}_{32}\text{O}_2$	2

Source: (Boateng *et al.*, 2016)

At present, one type of important derivative of coconut oil is fatty acid methyl ester that can be obtained from transesterification reaction. In these reactions, the triglycerides are converted step wise to diglycerides, monoglyceride and finally glycerol which sinks to the bottom and biodiesel which floats on top and can be siphoned off. The overall reaction of transesterification (Atabani *et al.*, 2012) can be written as Equation (8), Equation (9), and Equation (10) below:



Typical example of transesterification reaction from lauric acid as highest fatty acid content of coconut oil is presented in Figure 2.

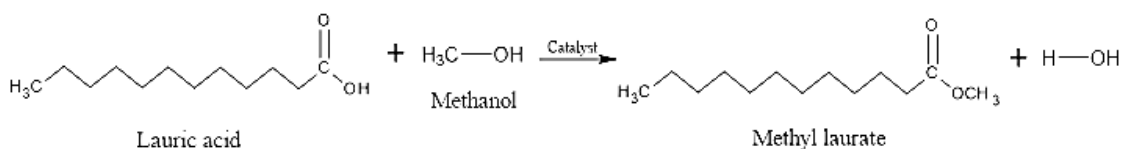


Figure 2. Transesterification of lauric acid into methyl laurate.

2.7.2. Nitrogen Compounds

Fatty Acid Methyl Esters (FAME) as product from transesterification reaction can be used as precursor for obtaining nitrogen compounds through an amidation process, which methyl ester is reacted with amine such as diethanolamine as shown in Figure 3. Catalyst is needed during amidation reaction, because diethanolamine and methyl ester are not reactive to each other. The commonly catalysts used in amidation reaction are NaOH, KOH, CaO, enzyme, and zeolites. In current study, catalyst used is zeolite-A.

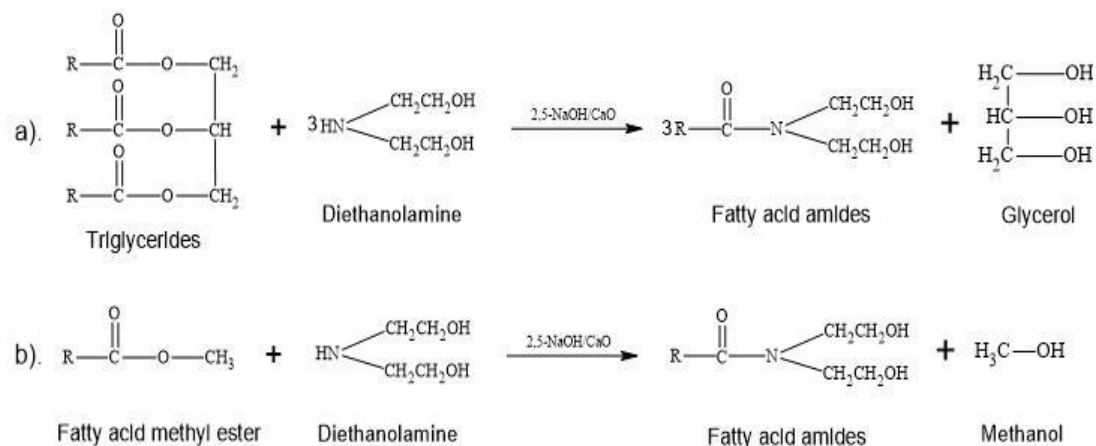


Figure 3. Amidation reaction from: a) fatty acid and b) methyl ester (Kumar and Ali, 2015).

2.8. Zeolite-A

Zeolites are crystalline aluminosilicates with a definite micropore structure. Primarily, zeolites are built from $[\text{SiO}_4]^{4-}$ and $[\text{AlO}_4]^{5-}$ tetrahedral which are infinitely extended in a three dimensional network that is linked together by a shared oxygen atom (Mgbemere *et al.*, 2017). Currently there are more than 200 types of zeolites, natural and synthetic, and they can be identified by their Silicon-Aluminium (Si/Al) ratio present in the atomic structure of the zeolite. One of synthetic zeolite is zeolite-A. Generally, structure of zeolite-A can be considered as inorganic polymer built from tetrahedral TO_4 units, where T is Si^{4+} or Al^{3+} ion. Each O atom is shared by two T atoms. The structure formula of zeolite is based on the crystallographic unit cell (Bekkum *et al.*, 1991). The structure of zeolite-A is shown in Figure 4.

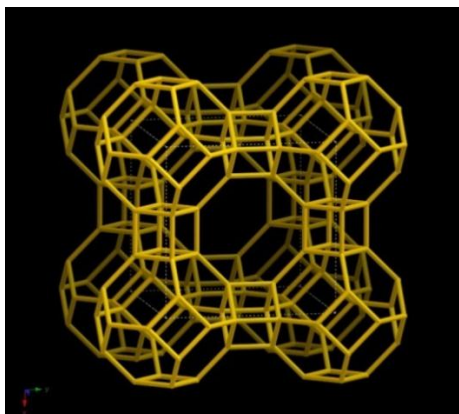


Figure 4. Structure of zeolite-A (Structure Commission of the International Zeolite Association (IZA-SC), 2017).

Zeolite-A is low silica synthetic zeolite with ratio of Si/Al = 1 and chemical formula $\text{Na}_{12}(\text{AlO}_2)_{12}(\text{SiO}_2)_{12} \cdot 27\text{H}_2\text{O}$. Characteristics of Zeolite-A are high concentration of cation, optimum adsorption properties, and with certain porosity allows it to have shape selectivity in acidic catalyst (Simanjuntak *et al.*, 2019). Zeolite-A pore size is about 4 Å, but the dimension of these pores is varied depending on the types of ion that can be exchanged. Analysis zeolite-A using SEM will show an image of a cubic crystal structure with a lattice parameter of 12,32 Å (Ayele *et al.*, 2016). Based on Structure Commission of the International Zeolite Association (IZA-SC), analysis zeolite-A using XRD give some distinctive characteristic peaks which are $2\theta = 7.18^\circ$, 10.16° , 12.44° , 16.10° , and 23.96° .

Zeolite-A can be prepared from different raw materials, such as sodium metasilicate and by-product from aluminum etching process (Hussar *et al.*, 2011), sodium silicate and sodium aluminate (Selim *et al.*, 2017), natural kaolin (Salih *et al.*, 2020), fumed silica and sodium aluminate (Isa *et al.*, 2018), and rice husk silica (Pandiangan *et al.*, 2019). In this study, zeolite-A was prepared from rice husk silica and food grade aluminum foil as an alternative precursor of alumina.

Zeolite-A is known to have varied applications, in which two of the most are as adsorbent and catalyst. As an adsorbent, zeolite-A has been utilized for the removal of several heavy metals from wastewater (Meng *et al.*, 2016). As the

catalyst, this particular zeolite has been utilized for transesterification to convert vegetable oil into biodiesel, which is known as another growing importance renewable liquid fuel (Pandiangan *et al.*, 2019). These varied utilizations have made zeolite-A an attractive material, drawing continuous interest for exploration of preparation techniques as well as the use of varied raw materials (Simanjuntak *et al.*, 2021).

2.9. Characterization of Products

2.9.1. X-Ray Diffraction (XRD)

X-ray diffraction is a common technique for the study of crystal structures and atomic spacing. In this study, analysis using XRD is used to investigate whether the zeolite-A is successfully produced. X-ray diffraction is based on constructive interference of monochromatic X-rays and a crystalline sample. These X-rays are generated by a cathode ray tube, filtered to produce monochromatic radiation, collimated to concentrate, and directed toward the sample (Ali *et al.*, 2022). The interaction of the incident rays with the sample produces constructive interference (and a diffracted ray) when conditions satisfy Bragg's law as shown in Equation (11) below:

$$n\lambda = 2d \sin \theta \quad (11)$$

Where n is an integer, λ is the wavelength of the X-rays, d is the interplanar spacing generating the diffraction, and θ is the diffraction angle. This law relates the wavelength of electromagnetic radiation to the diffraction angle and the lattice spacing in a crystalline sample. These diffracted X-rays are then detected, processed, and counted. By scanning the sample through a range of 2θ angles, all possible diffraction directions of the lattice should be attained due to the random orientation of the powdered material. The diffractometer system of XRD can be shown in Figure 5.

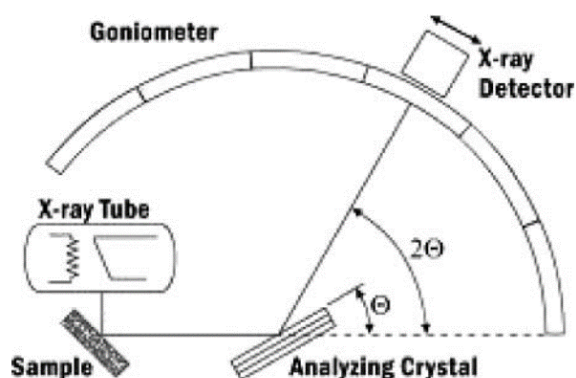


Figure 5. Schematic diagram of a diffractometer system (Bunaciu *et al.*, 2015).

The geometry of an X-ray diffractometer is such that the sample rotates in the path of the collimated X-ray beam at an angle θ while the X-ray detector is mounted on an arm to collect the diffracted X-rays and rotates at an angle of 2θ . The instrument used to maintain the angle and rotate the sample is termed a goniometer. In practice, XRD analysis will produce a diffractogram with unique diffraction pattern for each compound, in term of 2θ angle. An example is diffractogram of zeolite-A as presented in Figure 6.

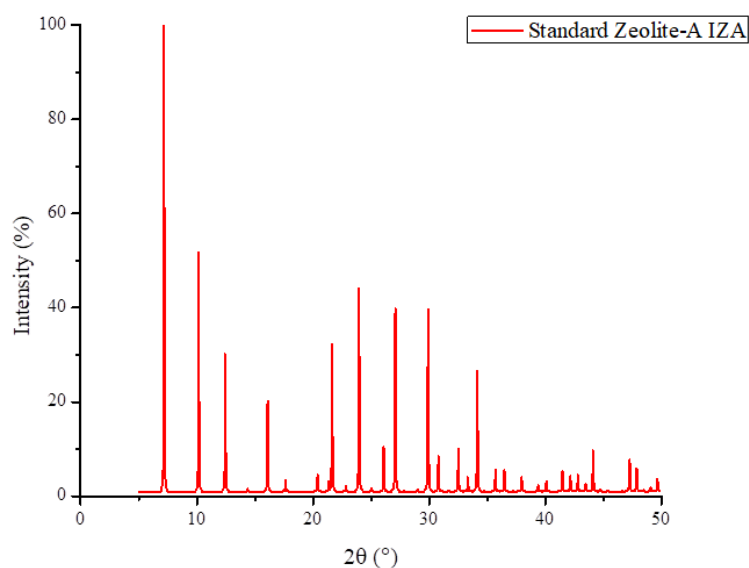


Figure 6. XRD Pattern of Zeolite-A (Structure Commission of the International Zeolite Association (IZA-SC), 2017).

2.9.2. Scanning Electron Microscopy with Energy Dispersive X-ray (SEM-EDX)

Scanning electron microscopy (SEM) has been used as an effective method in analysis of organic and inorganic materials on a nanometer to micrometer (μm) scale. In this study, SEM is used to analyze the surface morphology of zeolite-A catalyst and the morphology of the mild steel surface after exposure to corrosive solution in the absence and presence of a certain concentration of corrosion inhibitor. SEM works at a high magnification reaches to 300.000x and even 1.000.000 (in some modern models) in producing images very precisely of wide range of materials. Energy Dispersive X-ray (EDX) spectroscopy works together with SEM to provide qualitative and semi-quantitative results. Both techniques have the potential to introduce fundamental information on material composition of scanned specimens, which could not be provided by the common laboratory tests. The components of SEM can be seen in Figure 7.

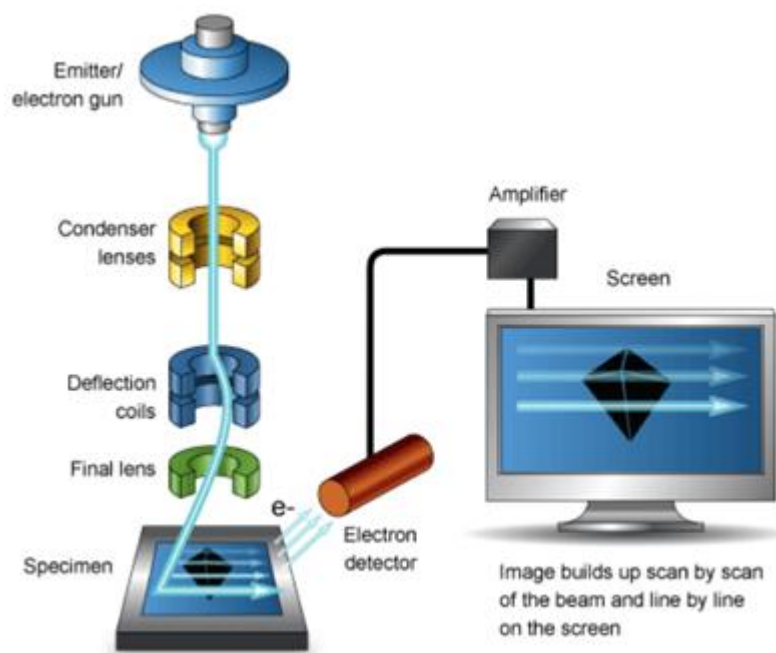


Figure 7. Scanning Electron Microscopy (SEM) components (Mohammed and Abdullah, 2018).

SEM imaging begins with an electron gun generating a beam of energetic electrons down the column onto a series of electromagnetic lenses. These lenses are tubes, wrapped in coil and referred to as solenoids. The coils are adjusted to focus the incident electron beam onto the specimen, and then the specimen emits an electron detector picks up the rebounding electrons and records their imprints. This information is translated onto a screen, and the operator will control the brightness and the intensity which allows three-dimensional images to be represented clearly. For an example, the cubic shape of zeolite-A can be detected by SEM as shown in Figure 8.

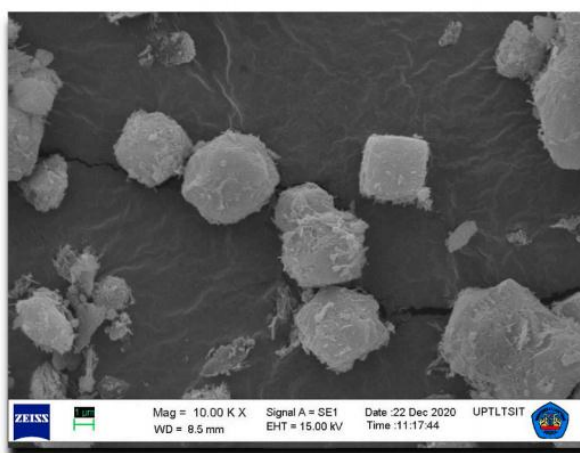


Figure 8. Micrograph of zeolite-A (Simanjuntak *et al.*, 2021).

2.9.3. Fourier Transform Infrared (FTIR)

Fourier Transform Infrared (FTIR) is one of the important analytical techniques for researchers. This type of analysis can be used for characterizing samples in the forms of liquids, solutions, pastes, powders, films, fibers, and gases (Fan *et al.*, 2012). Compared to other types of characterization analysis, FTIR is quite popular. This characterization analysis is quite rapid, good in accuracy, and relatively sensitive (Jaggi and Vij, 2006). FTIR spectroscopy is based on the principle that when a sample is probed with an infrared (IR) beam, the functional groups within that sample will absorb the IR radiation, and the vibrational

characteristics of each functional group will then be reflected (Bangaoil *et al.*, 2020).

Infrared spectroscopy measured the absorption of IR radiation made by each bond in the molecule and as a result produces spectrum which is commonly designated as % transmittance versus wavenumber (cm^{-1}). A diverse range of materials containing the covalent bond absorbed electromagnetic radiation in the IR region. IR spectrum is divided into three wavenumber regions: far-IR spectrum (less than 400 cm^{-1}), mid-IR spectrum ($400\text{-}4000 \text{ cm}^{-1}$), and near-IR spectrum ($4000\text{-}13000 \text{ cm}^{-1}$). The mid-IR spectrum is the most widely used in the sample analysis (Nandiyanto *et al.*, 2019). The specific frequency of each functional groups can be seen in Table 2.

Table 2. Range in wavenumber (cm^{-1}) of each functional groups

Wavenumber (cm^{-1})	Functional group
3200–3550	O–H stretching
3300–3500	N–H stretch, primary amine gives two, secondary one, while tertiary amine gives no peak
3500–3500	O=C–N–H stretch
2260–2220	Nitrile (CN)
2950–2850	C–H stretch
3010–3100	=C–H stretch
1620–1680	C=C stretch
1750–1730	Ester C=O
1780–1710	Carboxylic acid C=O
1690–1630	Amide C=O

Source: (Chen *et al.*, 2015)

The spectrum obtained from FTIR analysis is a correlation between intensity and frequency. Intensity shows the level number of component and wavenumber shows the type of bond in the components contained in a sample, as shown in Figure 9.

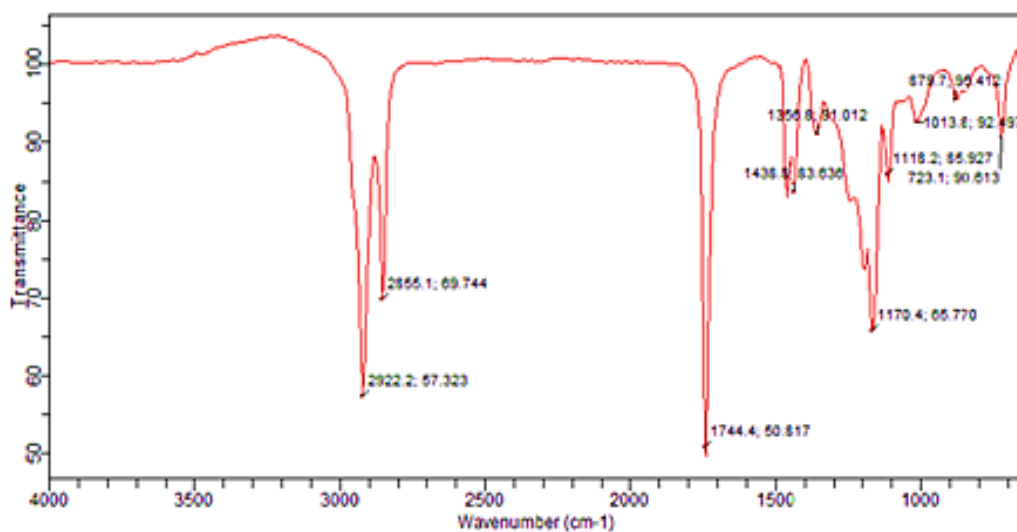


Figure 9. An example of FTIR spectrum of coconut oil methyl ester (Herliana *et al.*, 2021).

From FTIR analysis of methyl ester presented in Figure 9, it shows that the methyl ester was identified by the presence of sharp absorption peak at wavenumber 1744 cm^{-1} represents carbonyl (C=O) group, wavenumber at 1170 cm^{-1} represents C-O group, and absorption bands at 2922 cm^{-1} , 2855 cm^{-1} , and 1438 cm^{-1} are attributed to -C-H stretching and bending of the alkane group.

The typical FTIR spectrometer consists of an IR light source, interferometer, sample compartment, detector, amplifier, and computer. The light source generates radiation which strikes the sample passing through the interferometer and reaches the detector. Then the signal is amplified and converted to digital signal (interferogram) by the amplifier and analog-to-digital converter, respectively. Michelson interferometer is the main core of FTIR spectrometer and is shown in Figure 10.

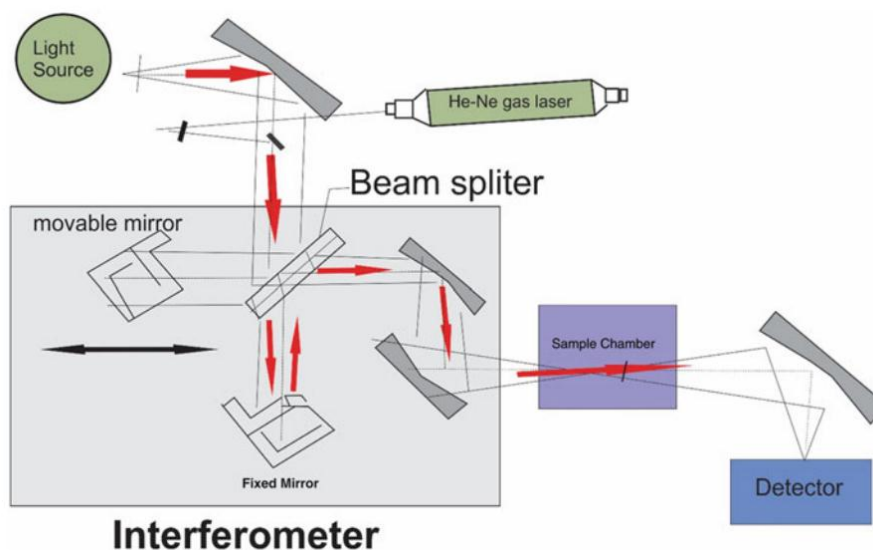


Figure 10. Instrumentation of the double-beam (top) and single-beam (bottom) IR spectrophotometers (Genzel *et al.*, 2008).

2.9.4. Gas Chromatography–Mass Spectrometry (GC–MS)

Gas Chromatography–Mass Spectrometry (GC–MS) is a combination of two different instruments, which are Gas Chromatography and Mass Spectrometry. Compounds are injected and separated based on their volatility by GC, followed with analysis using the MS part of the instrument where the compound is irradiated using an electron until it breaks into ions and move toward the detectors (Al-Bukhaiti *et al.*, 2017). GC–MS can be used for qualitative and quantitative analysis for volatile and semi-volatile organic compounds in various experimental samples. GC–MS is an effective tool to identify and quantify chemicals in a complex mixture (Al-Rubaye *et al.*, 2017). Some of technical fields using GC-MS analysis are perfume industry (Asten, 2002), food (Chiu and Kuo, 2020), pharmacy research (He *et al.*, 2016), forensic (Bridge *et al.*, 2018), and to detect chemical warfare agent (Li *et al.*, 2020). Scheme of GC–MS can be seen in Figure 11.

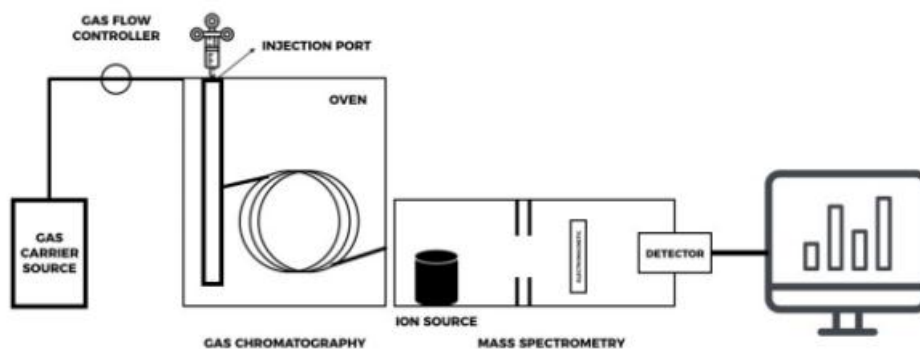


Figure 11. Scheme of GC–MS (Shubin and Lou, 2012).

The data is transferred to the computer until the chromatogram receives it. Data obtained are in the form of chromatogram comprised peaks, retention time and a peak area indicating the relative amount of the components (Darmapatni, 2016). In the GC chromatograms, each separated substance is represented by a peak. The number of peaks shows the number of separated compounds in the sample. The position of each peak shows the retention time for each compound. The mass spectrum is a graphical representation of the ion abundance versus the mass-to-charge ratio (m/z where m is the mass and z is the charge) of the ions separated in a mass spectrometer.

2.10. Corrosion Rate Measurement

Corrosion rate is the speed at which any metal in a specific environment deteriorates. It also can be defined as the amount of corrosion loss per year in thickness. The corrosion rate of a metallic material is evaluated by considering its density, equivalent weight and the area of exposed material (Afolabi *et al.*, 2014). Relative to metal density, exposed surface area, duration of exposure and some constant, the rate of corrosion of metal can be determined. Corrosion rate (CR) helps in understanding the vulnerability of metals to corrosion. Corrosion rate may be expressed in millimeter per year (mmpy) of metals degraded (Oparaodu and Okpokwasili, 2014). The rate of corrosion can be determined by weight loss method and electrochemical method.

2.10.1. Weight Loss Method (Wheel Test)

The most common method for estimating a corrosion rate is weight loss method (Umeozokwere *et al.*, 2016). In this method, the specimen of a given material (known as the coupon) is exposed to a process environment for a given duration of time. This specimen is then removed for analysis which begins with measurement to determine the weight loss taking place over the period of exposure. This is then expressed as corrosion rate (Usman *et al.*, 2015). The weight loss method is common used in industrial and laboratory scales because the equipment is simple and the results are quite accurate, but testing with the weight loss method for obtaining a corrosion rate has a disadvantage. The disadvantage of this method is can not detect changes quickly occurs during the corrosion process (Kumar *et al.*, 2014). The weight loss (W) and the corrosion rate (CR) were calculated by Equation (12) and Equation (13).

$$W = W_i - W_t \quad (12)$$

$$CR = \frac{10 \times W \times 365}{A \times D \times t} \quad (13)$$

Where W = weight loss (g), W_i = initial weight, W_t = end weight, CR = corrosion rate (mm.y^{-1} = millimeter per year), A = area of coupon (cm^2), D = density of metal (g.cm^{-3}) equal to 7.86 g.cm^{-3} for carbon steel, and t = time of exposure (days). The efficiency of inhibitors to reduce the corrosion rate for some metals were calculated by Equation (14).

$$\%P = \frac{(CR_0 - CR_i)}{CR_0} \times 100\% \quad (14)$$

Where $\%P$ = percent protection, CR_0 = corrosion rate without inhibitor, and CR_i = corrosion rate with inhibitor.

2.10.2. Electrochemical Methods

2.10.2.1. Electrochemical Impedance Spectroscopy (EIS) Measurement

EIS is one of the most important electrochemical techniques where the impedance in a circuit is measured by ohms (as resistance unit). EIS offers several

advantages reliant on the fact that it is a steady-state technique, that it utilizes small signal analysis, and that it is able to probe signal relaxations over a very wide range of applied frequency, from less than 1 mHz to greater than 1 MHz, using commercially available electrochemical working stations. EIS features is characterized by an electrical circuit that consists of resistances, capacitors, or constant phase elements that are connected in parallel or in a series to form an equivalent circuit, as shown in Figure 12.

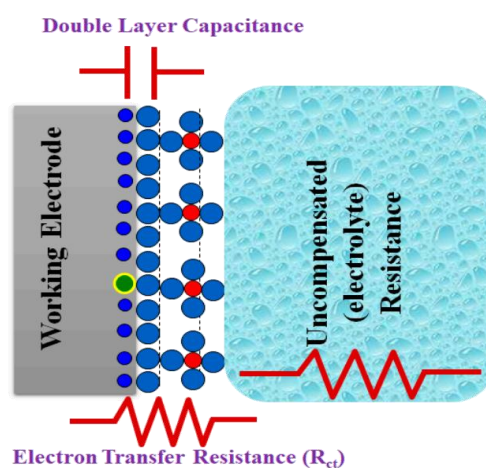


Figure 12. A scheme of EIS circuit and the redox reaction takes place at the surface of working electrodes in an electrochemical cell (Magar *et al.*, 2021).

The impedance expression is divided into a real part and an imaginary part. When the real part (Z_r) is plotted on the X-axis and the imaginary part (Z_i) is plotted on the Y-axis, a Nyquist Plot is formed (Figure 13). Each point on the Nyquist plot is an impedance value at a frequency point, while the Z_i is negative. At the X-axis, impedance at the right side of the plot is conducted with low frequency, while, at the higher frequencies, their generated impedances are exerted on the left. Moreover, on a Nyquist plot, impedance can be represented as a vector (arrow) of length $|Z|$. The angle between this arrow and the X-axis is called the phase angle (Wang *et al.*, 2021).

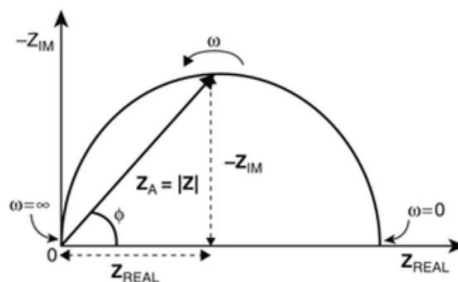


Figure 13. Nyquist plot with impedance vector (Lvovich, 2014).

In Nyquist plot, the intercept of the loops represent the charge transfer (R_{ct}). A larger R_{ct} indicates a stronger resistance to corrosion. Additionally, despite the similar appearance of the semicircles, the plots did not conform to a perfect semicircle. The deviation from an ideal semicircle is assumed to be attributed to inhomogeneity and roughness of the surface (Farag and El-din, 2012). The Nyquist plot obtained at open circuit potential (OCP) which consists of electrolyte resistance (R_s), charge transfer resistance (R_{ct}), and double layer capacitance as shown in Figure 14.

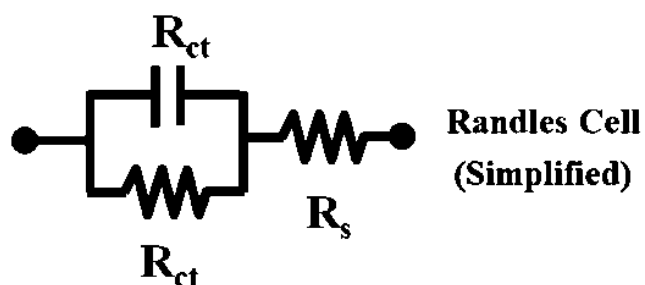


Figure 14. Electrochemical equivalent circuit used to fit the impedance spectra (Benavente, 2005).

The inhibition efficiency (% P) for EIS data was calculated by using Equation 14 (Zhang *et al.*, 2015).

$$\% P = \frac{(R_{ct(i)} - R_{ct(o)})}{R_{ct(i)}} \times 100\% \quad (14)$$

Where % P is inhibition efficiency in term of percent protection, $R_{ct(i)}$ is charge transfer resistance with inhibitor and $R_{ct(o)}$ is charge transfer without inhibitor.

2.10.2.2. Potentiodynamic Polarization (PDP) Measurement

Potentiodynamic polarization (PDP) measurement belongs to one of the most commonly used DC electrochemical method in corrosion measurements. The potential in a wide range is applied on the test electrode, due to which on the metal surface dominantly oxidation or reduction reaction happens (depending on the direction of polarization) and as a result, an adequate current is generated. The presentation of the potential in the function of current density (i) for each measured point results in obtaining the polarization curve. The polarization curve can be used to determine the corrosion potential and the corrosion rate of the metal. The electrochemical parameters obtained from processed polarization curves include the corrosion potential, E_{corr} (mV/SCE), the cathodic and anodic Tafel slopes β_c and β_a (mV dec^{-1}), and the corrosion current density (i_{corr}). The efficiencies of inhibitor were calculated using Equation 15 (Bentrah *et al.*, 2017).

$$\eta = \left(1 - \frac{i_{\text{corr}(0)}}{i_{\text{corr}}}\right) \times 100\% \quad (15)$$

Where η = protection efficiency of inhibitor (%), $i_{\text{corr}(0)}$ = corrosion current density with inhibitor and i_{corr} = current density without inhibitor.

The advantage of potentiodynamic polarization method is reflected in the possibility of a localized corrosion detection, easy and quick determination of the corrosion rate, and efficiency of the corrosion protection (Little *et al.*, 2007). An example of Tafel slope obtained from potentiodynamic polarization can be seen in Figure 15.

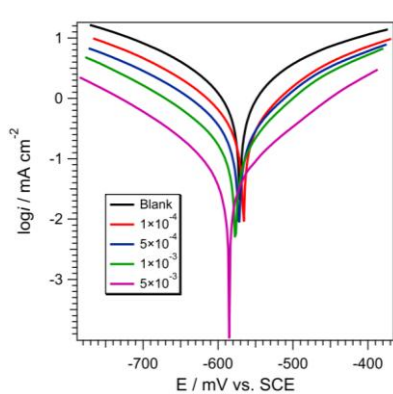


Figure 15. Tafel slope from potentiodynamic polarization (Farag *et al.*, 2018).

III. RESEARCH METHODS

3.1. Time and Places

This research was conducted on February – September 2022 in Laboratory of Inorganic/Physical Chemistry FMIPA University of Lampung. Characterization of Zeolite-A using XRD was carried out in Laboratory of Chemistry, Institut Teknologi Sepuluh Nopember (ITS), Surabaya, East Java. Characterization to identify chemical compounds using GC–MS of transesterification and amidation product was carried out in Laboratory of Chemistry, Universitas Islam Indonesia (UII), Yogyakarta. Functional group analysis using FTIR of transesterification and amidation product and Surface morphology analysis of zeolite-A catalyst and mild steel using SEM was carried out in Integrated Laboratory and Center for Technology Innovation (LTSIT), University of Lampung.

3.2. Materials and Instruments

Chemical used in this research were purchased from Merck include NaCl, NaOH, methanol, NaHCO₃, HNO₃, diethanolamine, Sb₂O₃, SnCl₂, HCl, mild steel (SAE/AISI Grade 1022) was purchased from Krakatau Steel, rice husk was obtained from local rice milling company, aluminum foil, food grade CO₂ gas, coconut oil, distilled water, pH indicator, filter paper, and silicon carbide paper with 200, 400, 600, 800, and 1200 grits.

Instruments used in this research were Fourier Transform Infrared (FTIR) NICOLET AVATAR 360, Gas Chromatography–Mass Spectrometry (GC–MS) Shimadzu GCMS-QP2010 SE, X-Ray Diffraction (XRD) PAN analytical type

EMPYREN, Scanning Electron Microscopy (SEM) ZEISS EVO 10, Polytetrafluoroethylene (PTFE) lined stainless steel autoclave, analytical balance METTLER AE 200, furnace, hotplate, mesh sieve, thermometer, magnetic stirrer, reflux condenser, micropipette, micrometer, and supporting glassware.

3.3 Research Procedures

3.3.1 Preparation of Rice Husk

Raw rice husk was obtained from a local rice milling industry in Untung Suropati, Bandar Lampung. Before use, the husk was soaked in water to remove the dirt. Floating husk was discharged, while sinking husk was collected, rinsed with distilled water, and then dried under the sunlight.

3.3.2. Extraction of Rice Husk Silica

To extract the silica, a mass of 50 g rice husk was mixed with 500 mL of 1.5% NaOH solution in a beaker glass. The mixture was boiled for 30 minutes, allowed to cool at room temperature, and then left for 24 hours. The mixture was filtered and the filtrate which contains silica (silica sol) collected. Production of solid silica was carried out by neutralization of the sol using HNO₃ 10% to produce a gel, followed by aging of the gel for 24 hours, and then repeat rinsing with distilled water to remove the excess of acid, and completed by oven drying of the gel 110 °C for 8 hours. Solid rice husk silica then grounded into powder and sieved with 325 mesh sieve to obtain the sample with homogeneous sizes.

3.3.3. Synthesis of Zeolite-A Catalyst

Zeolite-A was synthesized by preparing NaOH solution (20 grams in 200 mL of distilled water) and dissolved the 30 g of rice husk silica with a stirring speed of 500 rpm and heated at 70 °C for 3 hours. The sodium silicate solution obtained

then cooled and filtered using filter paper. The filtrate obtained was aged for 24 hours then added 13.5 grams of aluminum foil, stirred at 500 rpm for 3 hours. The resulting mixture was transferred into a Teflon lined autoclave for 24 hours aging process. After that, the mixture was crystallized in an oven at 100 °C for 96 hours. The gel obtained was filtered, washed with distilled water to pH of 7-8, then dried in an oven at 80 °C for 24 hours. The solid product was subjected to calcination treatment at 550 °C for 6 hours. To examine that the product is zeolite-A as expected, the zeolite-A obtained was characterized with X-Ray Diffraction (XRD) and Scanning Electron Microscopy (SEM).

3.3.4. Transesterification of Coconut Oil

Transesterification was carried out by ratio of the reactants 1 : 4, which 25 mL of coconut oil is reacted with 100 mL of methanol with the addition of 2.5 grams zeolite-A catalyst into a 250 mL round flask. The mixture then refluxed at 70 °C for 4 hours (Herliana *et al.*, 2021). The reflux product was cooled into room temperature, filtered with filter paper, put into a separating funnel, and left stand for one night. The glycerol was sink to the bottom and methyl ester was floated on top. To examine that the product is methyl ester as expected, the product was characterized using FTIR and GC-MS, and then used in the next procedure.

3.3.5. Reaction Between Methyl Ester and Diethanolamine

The purpose of reaction between methyl ester and diethanolamine was obtained nitrogen compounds and then used as corrosion inhibitor. Methyl ester and diethanolamine with same volume (20 mL) was placed in Teflon lined autoclave with addition of 2 grams zeolite-A catalyst, the mixture was heated at 80 °C for 24 hours and at 100°C for 24 and 48 hours. After the completion of experiment, the product was allowed to cool to room temperature, then filtered to remove zeolite-A catalyst. To examine that the product is nitrogen compound as expected, the

compounds obtained from this reaction was characterized using FTIR and GC–MS, and then used as corrosion inhibitor.

3.3.6. Preparation of Mild Steel

Mild steel used in this experiment was SAE/AISI Grade 1022 with the spectrographic analysis of the steel provided the chemical composition as shown in Table 3.

Table 3. Chemical composition of mild steel SAE/AISI Grade 1022

Element	Amount (%)
Fe	>98
C	0.22
Mn	0.74
Si	0.02
S	0.014
P	0.02
Ni	0.05
Mo	<0.01
Cu	<0.01
Al	<0.01

(Source: AS 1443)

Mild steel with the dimension of 2 x 1 x 0.1 cm was prepared and the surface of the metal was polished using silicon carbide paper with the size of 200, 400, 600, 800, and 1200 grits. The dimensions and weights of each coupon were accurately recorded.

3.3.7. Preparation of Solutions

The corrosive medium used was a brine solution 3 % (w/v) prepared by dissolving 30 g sodium chloride (NaCl) and 0.1 g sodium bicarbonate (NaHCO₃), in 1 L distilled water. The corrosive medium then saturated with food grade CO₂ gas at atmospheric pressure by purging the solution with the gas at a rate of approximately 150-200 mL min⁻¹. Inhibitor solution with the concentration of

15,000 ppm was prepared by dissolving 0.075 grams inhibitor (nitrogen compounds) in 5 mL methanol. The Clarke's solution was prepared by dissolving 5 g of SnCl_2 and 2 g of Sb_2O_3 in 100 mL concentrated HCl (Ilim *et al.*, 2021).

3.3.8. Corrosion Rate Measurement

Clean glass bottles (220 mL) were prepared to be used in the experiment. Four brine solutions with the same volume of 175 mL were prepared. One solution is used without addition of corrosion inhibitor, while the other three samples were used for the experiments with 150 ppm concentration of corrosion inhibitor. Each of the samples then purged for 45 minutes with CO_2 gas (at about 250 mL min^{-1}). A mild steel coupon prepared was placed to the bottles and the bottles were capped with crown seals and placed in a room temperature for 24 hours. After the completion of the experiment, the coupons was removed and immediately placed in Clarke's solution for 5 seconds in order to remove the corrosion product from the surface. The coupon was dipped into water for about 5 seconds, and into ethanol for another 5 seconds, and then dried and accurately weighed.

3.3.9. Scanning Electron Microscopy with Energy Dispersive X-Ray (SEM-EDX)

SEM-EDX analysis is used to examine the surface morphology of the mild steel surface after exposure to NaCl 3% in the absence and presence of a certain concentration of inhibitor for 24 hours. An untreated (original) coupon, a coupon immersed in brine solution without inhibitor, and a coupon immersed in brine solution containing inhibitor was analyzed their morphology using SEM-EDX.

V. CONCLUSIONS AND SUGGESTIONS

5.1. Conclusions

From the results obtained of this study, several conclusions were obtained as follows:

1. Synthesized zeolite-A has similar characteristic with standard zeolite-A IZA, based on analysis using XRD showed diffraction pattern in 2θ range $7-34^\circ$, and analysis using SEM showed the cubic structure on its crystal.
2. Zeolite-A has a good catalytic activity for transesterification and reaction between methyl ester and diethanolamine, indicated by formation of methyl ester coconut oil with distinctive aroma of methyl laurate and formation of nitrogen compounds.
3. FTIR analysis showed methyl ester as transesterification product was formed indicated by specific wavenumbers at 2922 cm^{-1} , 2855 cm^{-1} , and 1438 cm^{-1} are attributed to -C-H stretching and bending of the alkane group, wavenumbers at 1744 cm^{-1} is attributed to carbonyl (C=O) group and the absorption band at 1170 cm^{-1} represents C-O group. GC-MS analysis showed methyl laurate is the highest component (38.85%) in methyl ester as transesterification product.
4. FTIR analysis of nitrogen compounds showed that the reaction was successfully converted methyl ester into nitrogen compounds, indicated by absorption band at the wavenumber range of $3000-3750\text{ cm}^{-1}$ which represents N-H group, and also supported by wavenumber range of $1600-1630\text{ cm}^{-1}$. GC-MS analysis showed that P-3 as product reaction at 100°C for 48 hours has the highest amount of nitrogen compounds (53.54%).
5. Nitrogen compounds obtained from reaction at 100°C for 48 hours (P-3) showed the best activity as corrosion inhibitor on the experimental using wheel test method, indicated by the highest percent protection (97.9%). SEM

analysis for mild steel surface treated with P-3 as inhibitor also showed the inhibitor was well protected the surface from corrosion, and EDX analysis showed the existence of N atom on mild steel surface treated with P-3 as inhibitor indicated the formation of protective layer against corrosion.

5.2. Suggestions

Several suggestions given for the next study were shown in following points:

1. Optimizing the experimental condition for reaction between methyl ester and diethanolamine, such as doing the experiment with various ratio of reactants, temperature, and reaction time or using another catalyst for obtaining the higher amount of nitrogen compounds.
2. Testing the corrosion inhibitor compounds with another method such as Electrochemical Impedance Spectroscopy (EIS) and Tafel Polarization, and doing several repeated for obtaining higher accuracy of experimental data.

REFERENCES

- Adejo, S. O., Yiase, S. G., Leke, L., Onuche, M., Atondo, M. V., and Uzah, T. T. 2019. Corrosion Studies of Mild Steel in Sulphuric Acid Medium by Acidimetric Method. *Int. J. Corros. Scale Inhib.* 8(1): 50–61.
- Afolabi, A. S., Muhirwa, A. C., Abdulkareem, A. S., and Muzenda, E. 2014. Weight Loss and Microstructural Studies of Stressed Mild Steel in Apple Juice. *International Journal of Electrochemical Science.* 9(11):5 895–5906.
- Aghuy, A. A., Zakeri, M., Moayed, M. H., and Mazinani, M. 2015. Effect of Grain Size on Pitting Corrosion of 304L Austenitic Stainless Steel. *Corrosion Science.* 94: 368–376.
- Al-Bukhaiti, W. Q., Noman, A., Qasim, A. S., and Al-Farga, A. 2017. Gas Chromatography: Principles, Advantages and Applications in Food Analysis. *International Journal of Agriculture Innovations and Research.* 6(1): 2319–2327.
- Al-Rubaye, A. F., Hameed, I., and Kadhim, M. J. 2017. A Review: Uses of Gas Chromatography-Mass Spectrometry (GC-MS) Technique for Analysis of Bioactive Natural Compounds of Some Plants. *International Journal of Toxicological and Pharmacological Research.* 9(1): 81–85.
- Ali, A., Chiang, Y. W., and Santos, R. M.. 2022. X-Ray Diffraction Techniques for Mineral Characterization : A Review for Engineers of the Fundamentals , Applications, and Research Directions. *Minerals.* 12(205):1–25.
- Alvarez, P. E., Fiori-bimbi, M. V., Neske, A., Brandán, S. A., and Gervasi, C. A. 2017. Rollinia Occidentalis Extract as Green Corrosion Inhibitor for Carbon Steel in HCl Solution. *Journal of Industrial and Engineering Chemistry.* 9(17): 165–175.
- Asmara, Y. P., Kurniawan, T., Geter, A., Sutjipto, E., and Jafar, J. 2018. Application of Plants Extracts as Green Corrosion Inhibitors for Steel in Concrete - A Review. *Indonesian Journal of Science & Technology.* 3(2):158–170.
- Asten, V. A. 2002. The Importance of GC and GC-MS in Perfume Analysis. *TrSC - Trends in Analytical Chemistry.* 21(9): 698–708.
- Atabani, A. E., Silitonga, A. S., Badruddin, I. A., Mahlia, T. M. I., Masjuki, H. H.,

- and Mekhilef, S. 2012. A Comprehensive Review on Biodiesel as an Alternative Energy Resource and Its Characteristics. *Renewable and Sustainable Energy Reviews*. 16(4): 2070–2093.
- Ayele, L., Perez-Pariente, J., Chebude, Y., and Diaz, I. 2016. Synthesis of Zeolite A Using Kaolin from Ethiopia and Its Application in Detergents. *New J. Chem.* 40: 3440–2446.
- Bangaoil, R., Santillan, A., Angeles, L. M., Abanilla, L., Lim, A., Ramos, M. C., Fellizar, A., Guevarra, L., and Albano, M. 2020. ATR-FTIR Spectroscopy as Adjunct Method to the Microscopic Examination of Hematoxylin and Eosin-Stained Tissues in Diagnosing Lung Cancer. *PLoS ONE*. 15(5): 1–15.
- Bekkum, V. H., Flanigen, E. M., Jacobs, P. A., and Jansen, J. C. 1991. *Introduction to Zeolite Science and Practice*. 2nd ed. Elsevier. Amsterdam.
- Benavente, J. 2005. Electrochemical Impedance Spectroscopy as a Tool for Electrical and Structural Characterizations of Membranes in Contact with Electrolyte Solutions. Pages 463–471 in *Recent Advances in Multidisciplinary Applied Physics*. Elsevier. Oxford.
- Bentrah, H., Chala, A., Djellab, M., Rahali, Y., and Taoui, H. 2017. The Influence of Temperature on the Corrosion Inhibition of API 5L X42 Pipeline Steel in HCl Medium by Gum Arabic. *Anti-Corrosion Methods and Materials*. 64(4): 1–21.
- Boateng, L., Ansong, R., Owusu, W. B., and Steiner-Asiedu, M. 2016. Coconut Oil and Palm Oil's Role in Nutrition, Health and National Development: A Review. *Ghana Medical Journal*. 50(3): 189–196.
- Bridge, C., Maric, M., and Jones, K. 2018. GC× GC–MS for Forensic Analysis. *The Column*. 14(12): 25–31.
- Bunaciu, A. A., Udristioiu, E. G., and Aboul-Enein, H. Y. 2015. X-Ray Diffraction : Instrumentation and Applications. *Critical Reviews in Analytical Chemistry*. 45(4): 289–299.
- Chen, D., Han, E. H., and Wu, X. 2016. Effects of Crevice Geometry on Corrosion Behavior of 304 Stainless Steel during Crevice Corrosion in High Temperature Pure Water. *Corrosion Science*. 111(16): 518–530.
- Chen, Y., Zou, C., Mastalerz, M., Hu, S., Gasaway, C., and Tao, X. 2015. Applications of Micro-Fourier Transform Infrared Spectroscopy (FTIR) in the Geological Sciences-a Review. *International Journal of Molecular Sciences*. 16: 30223–30250.
- Chiu, H. H. and Kuo, C. H. 2020. Gas Chromatography-Mass Spectrometry-Based Analytical Strategies for Fatty Acid Analysis in Biological Samples. *Journal in Food and Drug Analysis*. 28(1): 60–73.

- Costa, M. and Klein, C. B. 2006. Toxicity and Carcinogenicity of Chromium Compounds in Humans. *Critical Reviews in Toxicology*. 36(2): 155–163.
- Darmapatni, K. A. G. 2016. Pengembangan Metode GC-MS Untuk Penetapan Kadar Acetaminophen Pada Spesimen Rambut Manusia. *Jurnal Biosains Pascasarjana*. 18(3): 13–17.
- Dwivedi, D., Lepkova, K., and Becker, T. 2017. Carbon Steel Corrosion: A Review of Key Surface Properties and Characterization Methods. *Royal Society of Chemistry*. 7:4580–4610.
- Fan, M., Dai, D., and Huang, B. 2012. Fourier Transform Infrared Spectroscopy for Natural Fibres. *Fourier Transform - Materials Analysis. In Tech*. ISBN: 978-953-51-0594-7
- Farag, A. A., Ismail, A. S., and Migahed, M. A. 2018. Environmental-Friendly Shrimp Waste Protein Corrosion Inhibitor for Carbon Steel in 1 M HCl Solution. *Egyptian Journal of Petroleum*. 27(4): 1187–1194.
- Farag, A. A. and Noor El-Din, M. R. 2012. The Adsorption and Corrosion Inhibition of Some Nonionic Surfactants on API X65 Steel Surface in Hydrochloric Acid. *Corrosion Science*. 64: 174–183.
- Fontana, M. G. 2000. *Corrosion Engineering*. Mc-Graw Hill. New York.
- Garai, S., Garai, S., Jaisankar, P., Singh, J. K., and Elango, A. 2012. A Comprehensive Study on Crude Methanolic Extract of *Artemisia Pallens* (Asteraceae) and Its Active Component as Effective Corrosion Inhibitors of Mild Steel in Acid Solution. *Corrosion Science*. 60:193–204.
- Genzel, R., Lutz, D., Sturm, E., Egami, E., Kunze, D., Moorwood, A., Rigopoulou, D., Spoon, H., Strenberg, A., and Tacconi-Garman, L. 2008. What Powers Ultraluminous IRAS Galaxies? *The Astrophysical Journal*. 458(579): 65–78.
- Goyal, M., Kumar, S., Bahadur, I., Verma, C., and Ebenso, E. E. 2018. Organic Corrosion Inhibitors for Industrial Cleaning of Ferrous and Non-Ferrous Metals in Acidic Solutions: A Review. *Journal of Molecular Liquids*. 256(2017): 565–573.
- Håkansson, E., Hoffman, J., Predecki, P., and Kumosa, M. 2017. The Role of Corrosion Product Deposition in Galvanic Corrosion of Aluminum/Carbon Systems. *Corrosion Science*. 114: 10–16.
- He, M., Yang, Z. Y., Guan, W. N., Goncalves, V. C. M., Nie, J., and Wu, H. 2016. GC-MS Analysis and Volatile Profile Comparison for the Characteristic Smell from Liang-Wai Gan Cao (*Glycyrrhiza Uralensis*) and Honey-Roasting Products. *Journal of Chromatographic Science*. 54(6):879–887.

- Helmi, M., Ghadiri, M., Tahvildari, K., and Hemmati, A. 2021. Biodiesel Synthesis Using Clinoptilolite-Fe₃O₄-Based Phosphomolybdic Acid as a Novel Magnetic Green Catalyst from *Salvia Mirzayanii* Oil via Electrolysis Method: Optimization Study by Taguchi Method. *Journal of Environmental Chemical Engineering*. 9(105988): 1–11.
- Herliana. 2022. Konversi Metil Ester Asam Lemak Minyak Kelapa Menjadi Senyawa Amida Menggunakan Dietanolamina Dan Uji Aplikasinya Sebagai Inhibitor Korosi. *Skripsi*. Universitas Lampung.
- Herliana, H., Ilim, I., Simanjuntak, W., and Pandiangan, K. D. 2021. Transesterification of Coconut Oil (*Cocos Nucifera* L.) into Biodiesel Using Zeolite-A Catalyst Based on Rice Husk Silica and Aluminum Foil. *Journal of Physics: Conference Science*. 1751(012091): 1–8.
- Hussar, K., Teekasap, S., and Somsuk, N. 2011. Synthesis Zeolite A from By-Product of Aluminum Etching Process: Effects of Reaction Temperature and Reaction Time on Pore Volume. *American Journal of Environmental Sciences*. 7(1): 35–42.
- Ilim, I., Bahri, S., Marjunus, R., and Simanjuntak, W. 2021. The Effect of Initiator Concentrations on Corrosion Inhibition Activity of Polymeric Derivatives of 2-Vinylpyridin. *Journal of Physics: Conference Series*. 1751(1): 1–7.
- Ilim, I., Bahri, S., Simanjuntak, W., Syah, Y. M., Bundjali, B., and Buchari, B. 2017. Performance of Oligomer 4-Vinylpiperidine as a Carbon Dioxide Corrosion Inhibitor of Mild Steel. *Journal of Materials and Environmental Science*. 8(7): 2381–2390.
- Ilim, I., Fitriani, R., Prabowo, T., Bahri, S., Marjunus, R., and Simanjuntak, W. 2021. Molecular Weight Distribution and Corrosion Inhibitor Activity of 4-Vinylpyridine Oligomer Synthesized Using Low Concentration Hydrogen Peroxide as the Initiator. *International Journal of Corrosion and Scale Inhibition*. 10(1): 284–301.
- Ilim, I., Jefferson, A., Simanjuntak, W., Jeannin, M., Syah, Y. M., Bundjali, B., and Buchari, B. 2016. Synthesis and Characterization of Oligomer 4-Vinylpyridine as a Corrosion Inhibitor for Mild Steel in CO₂ Saturated Brine Solution. *Indonesian Journal of Chemistry*. 16(2): 198–207.
- Isa, M. A., Chew, T. L., and Yeong, Y. F.. 2018. Zeolite NaY Synthesis by Using Sodium Silicate and Colloidal Silica as Silica Source. *Journal of Physics: Conference Science*. 458(012001): 1–8.
- IZA. 2017. Framework Type LTA. *International Zeolite Association*. <https://asia.iza-structure.org/IZA-SC/framework.php?STC=LTA>.
- Jaggi, N. and Vij, D. 2006. *Fourier Transform Infrared Spectroscopy. Handbook of Applied Solid State Spectroscopy*. Springer. Boston.

- Jiang, L., Qiang, Y., Lei, Z., Wang, J., Qin, Z., and Xiang, B. 2018. Excellent Corrosion Inhibition Performance of Novel Quinoline Derivatives on Mild Steel in HCl Media: Experimental and Computational Investigations. *Journal of Molecular Liquids*. 133(10): 1–30.
- Kahyarian, A., Achour, M., and Nestic, S. 2017. CO₂ Corrosion of Mild Steel. *Trends in Oil and Gas Corrosion Research and Technologies*. Elsevier. Ohio.
- Khan, I. U., Yan, Z., and Chen, J. 2020. Production and Characterization of Biodiesel Derived From a Novel Source *Koelreuteria Paniculata* Seed Oil. *Energies*. 13(791): 1–16.
- Koushik, B. G., Steen, N. V. D., Mamme, M. H., Ingelgem, Y. V., and Terryn, H. 2021. Review on Modelling of Corrosion under Droplet Electrolyte for Predicting Atmospheric Corrosion Rate. *Journal of Materials Science and Technology*. 62: 254–267.
- Kumar, D. and Ali, A. 2015. Direct Synthesis of Fatty Acid Alkanolamides and Fatty Acid Alkyl Esters from High Free Fatty Acid Containing Triglycerides as Lubricity Improvers Using Heterogenous Catalyst. *Fuel*. 159: 845–853.
- Kumar, N., Singh, A., Kumar, A., and Patel, S. 2014. Corrosion Behaviour Of Austenitic Stainless Steel Grade 316 In Strong Acid Solution. *International Journal of Advance Research*. 2(5): 1–9.
- Kuruvila, R., Kumaran, S. T., Khan, M. A., and Uthayakumar, M. 2018. A Brief Review on the Erosion-Corrosion Behavior of Engineering Materials. *Corrosion Rev.* 10(1515): 1–13.
- Li, B., Kong, J., Yang, L., Zhang, L., Zhang, Z., and Li, C. 2020. Direct Detection of Chemical Warfare Agent Simulants in Soil by Thermal Desorption-Low Temperature Plasma-Mass Spectrometry. *International Journal of Mass Spectrometry*. 451: 1–9.
- Little, B. J., Mansfeld, F. B., Arps, J., and Earthman, J. C. 2007. Microbiologically Influenced Corrosion. in *Encyclopedia at Electrochemistry*. Willey. Weinheim.
- Locke, C. E. 1997. *ASM Handbook: Vol 13 Corrosion*. ASM International. Almere.
- Lvovich, V. F. 2014. Electrochemical Impedance Spectroscopy (EIS) Applications to Sensors and Diagnostics. in *Encyclopedia of Applied Electrochemistry*. Springer. New York.
- Magar, H. S., Hassan, R. Y. A., and Mulchandani, A. 2021. Electrochemical Impedance Spectroscopy (Eis): Principles, Construction, and Biosensing Applications. *Sensors*. 21(19): 1–21.

- Meng, Q., Chen, H., Lin, J., Lin, Z., and Sun, J. 2017. Zeolite A Synthesized from Alkaline Assisted Pre-Activated Halloysite for Efficient Heavy Metal Removal in Polluted River Water and Industrial Wastewater. *Journal of Environmental Sciences*. 56(6): 254–262.
- Mgbemere, H. E., Ekpe, I., and Lawal, G. I. 2017. Zeolite Synthesis, Characterisation and Application Areas: A Review. *International Research Journal of Environmental Sciences*. 6(10):45–59.
- Mohammed, A. and Abdullah, A. 2018. Scanning Electron Microscopy (SEM): A Review. *International Conference on Hydraulics and Pneumatics - HERVEX*. 11(7):1–9.
- Musa, A. Y., Jalgham, R. T. T., and Mohamad, A.B. 2012. Molecular Dynamic and Quantum Chemical Calculations for Phthalazine Derivatives as Corrosion Inhibitors of Mild Steel in 1M HCl. *Corrosion Science*. 56: 176–183.
- Nandiyanto, A.B. D., Oktiani, R., and Ragadhita, R. 2019. How to Read and Interpret FTIR Spectroscopy of Organic Material. *Indonesian Journal of Science & Technology*. 4(1): 97–118.
- Narayanankutty, A., Illam, S. P., and Raghavamenon, A. C. 2018. Health Impacts of Different Edible Oils Prepared from Coconut (Cocos Nucifera): A Comprehensive Review. *Trends in Food Science and Technology*. 80: 1–7.
- Oparaodu, K. O. and Okpokwasili, G. C. 2014. Comparison of Percentage Weight Loss and Corrosion Rate Trends in Different Metal Coupons from Two Soil Environments. *International Journal of Environmental Bioremediation & Biodegradation*. 2(5): 243–249.
- Pampliega, A.A., Hauffman, T., Petrova, M., Breugelmansa, T., Muselle, T., Bergh, K. V., De Strycker, J., Terryn, H., and Hubin, A. 2014. Corrosion Study on Al-Rich Metal-Coated Steel by Odd Random Phase Multisine Electrochemical Impedance Spectroscopy. *Electrochimica Acta*. 124(9): 165–175.
- Pandiangan, K. D., Simanjuntak, W., Pratiwi, E., and Rilyanti, M. 2019. Characteristics and Catalytic Activity of Zeolite-a Synthesized from Rice Husk Silica and Aluminium Metal by Sol-Gel Method. *Journal of Physics: Conference Series*. 1338(012015): 1–9.
- Qiang, Y., Zhang, S., Tan, B., and Chen, S. 2018. Evaluation of Ginkgo Leaf Extract as an Eco-Friendly Corrosion Inhibitor of X70 Steel in HCl Solution. *Corrosion Science*. 2017: 1-17.
- Roy, P., Karfa, P., Adhikari, U., and Sukul, D. 2014. Corrosion Inhibition of Mild Steel in Acidic Medium by Polyacrylamide Grafted Guar Gum with Various Grafting Percentage: Effect of Intramolecular Synergism. *Corrosion Science*.

88: 246–253.

- Rufino, M. S. M., Alves, R. E., de Brito, E. S., Pérez-Jiménez, J., Saura-Calixto, F., and Mancini-Filho, J. 2010. Bioactive Compounds and Antioxidant Capacities of 18 Non-Traditional Tropical Fruits from Brazil. *Food Chemistry*. 121(4): 996–1002.
- Salarvand, Z., Amirnasr, M., Talebian, M., Raeissi, K., and Meghdadi, S. 2016. Enhanced Corrosion Resistance of Mild Steel in 1M HCl Solution by Trace Amount of 2-Phenyl-Benzothiazole Derivatives: Experimental, Quantum Chemical Calculations and Molecular Dynamics (MD) Simulation Studies. *Case Studies in Fire Safety*. 11(2): 1–52.
- Salih, A. M., Williams, C., and Khanaqa, P. A. 2020. Synthesis of Zeolite A from Iraqi Natural Kaolin Using a Conventional Hydrothermal Synthesis Technique. *UKH Journal of Science and Engineering*. 4(2): 11–23.
- Sari, F., Susanto, B. H., and Bismo, S. 2018. The Potential Utilization of Coconut Oil and Palm Oil as Raw Material of Alkanolamide under Alkaline Conditions. *IOP Conference Series: Earth and Environmental Science*. 105(1): 1–6.
- Selim, M. M., El-Mekkawi, D. M., Aboelenin, R. M. M., Ahmed, S. A. S. A., and Mohamed, G. M. 2017. Preparation and Characterization of Na-A Zeolite from Aluminum Scrub and Commercial Sodium Silicate for The Removal Cd^{2+} From Water. *Journal of The Association of Arab Universities for Basic and Applied Sciences*. 24: 19–25.
- Shubin, W. G. L. and Lou, R. 2012. Applications of Chromatography Hyphenated Techniques in the Field of Lignin Pyrolysis. *Applications of Gas Chromatography*. 41(7): 1–17.
- Simanjuntak, W., Pandiangan, K. D., Sembiring, Z., and Simanjuntak, A. 2019. Liquid Fuel Production by Zeolite-A Catalyzed Pyrolysis of Mixed Cassava Solid Waste and Rubber Seed Oil. *Oriental Journal of Chemistry*. 35(1): 71–76.
- Simanjuntak, W., Pandiangan, K. D., Sembiring, Z., Simanjuntak, A., and Hadi, S. 2021. The Effect of Crystallization Time on Structure, Microstructure, and Catalytic Activity of Zeolite-A Synthesized from Rice Husk Silica and Food-Grade Aluminum Foil. *Biomass and Bioenergy*. 148(106050): 1–7.
- Tamalmani, K. and Husin, H. 2020. Review on Corrosion Inhibitors for Oil and Gas Corrosion Issues. *Applied Science*. 10(3389): 1–16.
- Tator, K. B. 1997. *Organic Coatings and Linings: ASM Handbook*. 9th Edition. ASM International. Almere,
- Umeozokwere, A. O., Ikenna, M., Ufuma, O. B., and Ezemuo, D. T. 2016. Corrosion Rates and Its Impact on Mild Steel in Some Selected

- Environments. *Journal of Scientific and Engineering Research*. 3(1): 34–43.
- Usman, A. D., Adams, F. V., and Okoro, L. 2015. Weight Loss Corrosion Study of Some Metals in Acid Medium. *Journal of Advances in Chemistry*. 11(2): 2–9.
- Verma, C., Ebenso, E. E., and Quraishi, M. A. 2019. Alkaloids as Green and Environmental Benign Corrosion Inhibitors : An Overview. *Int. J. Corros. Scale Inhib.* 8(3): 512–528.
- Wang, S., Zhang, J., Gharbi, O., Vivier, V., Gao, M., and Orazem, M. E. 2021. Electrochemical Impedance Spectroscopy. *Nature Reviews Methods Primers*. 41(1): 1–21.
- Yanuar, A. P., Pratikno, H., and Titah, H. S. 2017. Pengaruh Penambahan Inhibitor Alami Terhadap Laju Korosi Pada Material Pipa Dalam Larutan Air Laut Buatan. *Jurnal Teknik ITS*. 5(2): 8–13.
- Zhang, H. H., Pang, X., Zhou, M., Liu, C., Wei, L., and Gao, K. 2015. The Behavior of Pre-Corrosion Effect on the Performance of Imidazoline-Based Inhibitor in 3 Wt.% NaCl Solution Saturated with CO₂. *Applied Surface Science*. 356: 63–72.
- Zhang, X., Zhou, X., Hashimoto, T., and Liu, B. 2017. Localized Corrosion in AA2024-T351 Aluminium Alloy: Transition from Intergranular Corrosion to Crystallographic Pitting. *Materials Characterization*. 130(5): 230–236.